International Journal of Medical and Pharmaceutical Research

Online ISSN-2958-3683 | Print ISSN-2958-3675
Frequency: Bi-Monthly
Available online on: https://ijmpr.in/

Original Article

Multiparametric MRI (DWI, PWI, MRS) in the Characterization of Intracranial Tumors: A Prospective Observational Study

Sanjay Kumar Yadaw[1], Pankaj Banode[2], Gaurav Vedprakash Mishra[3]

[1] Senior Resident, Department of Radiodiagnosis, Jawaharlal Nehru Medical College, Datta Meghe Institute of Higher Education and Research (Deemed to be University), Sawangi (Meghe), Wardha, Maharashtra – 442001, India

[2] Professor and Head, Department of Radiodiagnosis, Jawaharlal Nehru Medical College, Datta Meghe Institute of Higher Education and Research (Deemed to be University), Sawangi (Meghe), Wardha, Maharashtra – 442001, India

[3] Professor, Department of Radiodiagnosis, Jawaharlal Nehru Medical College, Datta Meghe Institute of Higher Education and Research (Deemed to be University), Sawangi (Meghe), Wardha, Maharashtra – 442001, India

OPEN ACCESS

Corresponding Author:

Dr. Sanjay Kumar Yadaw
MBBS, MD, FVIR Senior Resident, Department of Radiodiagnosis, Email: sanjumdradio@gmail.com

Received: 28-02-2025
Accepted: 16-03-2025
Available online: 30-04-2025

ABSTRACT

Background: Conventional magnetic resonance imaging (MRI) provides excellent anatomical detail of intracranial space-occupying lesions but is often limited in differentiating tumor types and predicting histological grade. Advanced MRI techniques — diffusion-weighted imaging (DWI), perfusion-weighted imaging (PWI) and magnetic resonance spectroscopy (MRS) — provide complementary physiological and metabolic information. The present study was undertaken to evaluate the diagnostic value of multiparametric MRI in characterizing intracranial tumors and differentiating among major histological subtypes, with histopathology as the reference standard.

Materials and Methods: A prospective observational study was conducted in the Department of Radiodiagnosis, Jawaharlal Nehru Medical College, DMIMS (DU), Sawangi (Meghe), Wardha, between February 2024 to December 2025. Sixty consecutive patients with intracranial space-occupying lesions detected on conventional MRI were evaluated on a 1.5-Tesla scanner using a standardized multiparametric protocol that included DWI with apparent diffusion coefficient (ADC) mapping, dynamic susceptibility contrast (DSC) PWI with relative cerebral blood volume (rCBV) computation, and single-voxel/multi-voxel proton MRS for choline (Cho), creatine (Cr), N-acetylaspartate (NAA), lipid and lactate quantification. The imaging diagnosis was correlated with histopathological diagnosis after surgery or stereotactic biopsy. Sensitivity, specificity, accuracy and the area under the receiver-operating-characteristic curve (AUROC) were calculated for individual sequences and for the combined multiparametric approach.

Results: Of 60 patients (mean age 48.6 ± 14.7 years; M:F = 1.4:1), histopathology confirmed high-grade glioma (HGG) in 18 (30.0%), low-grade glioma (LGG) in 10 (16.7%), meningioma in 14 (23.3%), metastasis in 10 (16.7%), primary CNS lymphoma in 4 (6.7%) and miscellaneous tumors (schwannoma, pituitary adenoma, hemangioblastoma) in 4 (6.7%). Mean ADC was significantly lower in HGG ($0.78 \pm 0.12 \times 10^{-3}$ mm²/s) and lymphoma ($0.62 \pm 0.09 \times 10^{-3}$ mm²/s) than in LGG ($1.32 \pm 0.18 \times 10^{-3}$ mm²/s) ($p < 0.001$). Mean rCBV was highest in meningioma (6.12 ± 1.85) and HGG (4.82 ± 1.34), and significantly lower in LGG (1.46 ± 0.42) ($p < 0.001$). MRS demonstrated elevated Cho/Cr (>2.0) in all malignant tumors; HGG showed Cho/Cr 3.42 ± 0.88 with lipid–lactate peaks, while meningioma exhibited a characteristic alanine doublet at 1.48 ppm. The combined multiparametric protocol achieved a diagnostic accuracy of 92.5% (sensitivity 93.2%, specificity 91.5%, AUROC 0.94), significantly higher than DWI alone (75.0%), PWI alone (78.3%) or MRS alone (80.0%) ($p < 0.05$).

Conclusion: Multiparametric MRI integrating DWI, PWI and MRS substantially improves the pre-operative characterization of intracranial tumors and the differentiation between high-grade and low-grade lesions. The combined approach should be incorporated into routine neuro-oncological imaging protocols to guide biopsy targeting, surgical planning and treatment selection.

***Keywords**: Multiparametric MRI; Diffusion-Weighted Imaging; Perfusion-Weighted Imaging; Magnetic Resonance Spectroscopy; Intracranial Tumors; Glioma; Meningioma; Apparent Diffusion Coefficient; Cerebral Blood Volume.*

INTRODUCTION

Intracranial tumors constitute a heterogeneous group of neoplasms with widely differing biological behaviour, treatment strategies and prognoses. They account for approximately 1–2% of all malignancies but are responsible for disproportionately high morbidity and mortality because of their location and the limited regenerative capacity of the central nervous system. According to recent epidemiological data, the worldwide age-standardized incidence of primary brain tumors ranges between 7 and 11 per 100,000 population, with gliomas, meningiomas and pituitary tumors being the most common primary lesions, while metastases remain the most frequent intracranial neoplasms in adults overall [1].

Magnetic resonance imaging (MRI) is the imaging modality of choice for the detection, characterization and follow-up of intracranial tumors. Conventional MRI sequences — T1-weighted, T2-weighted, fluid-attenuated inversion recovery (FLAIR) and post-contrast T1-weighted images — provide excellent depiction of tumor location, size, mass effect, peritumoral edema and pattern of contrast enhancement. However, conventional sequences depict mainly the structural and morphological aspects of a lesion, and a substantial overlap exists in the appearance of various tumor types and grades [11,14]. Differentiating high-grade glioma from solitary metastasis, primary CNS lymphoma or atypical meningioma; distinguishing low-grade from high-grade glioma; and separating tumor recurrence from radiation necrosis are recognized diagnostic dilemmas where conventional imaging alone is frequently inadequate.

To overcome these limitations, advanced or "physiological" MRI techniques have been progressively integrated into neuro-oncological imaging. Diffusion-weighted imaging (DWI) and the derived apparent diffusion coefficient (ADC) maps assess the random motion of water molecules in tissue and have been shown to correlate inversely with cellular density [3,4]. Highly cellular tumors such as high-grade gliomas, lymphomas and small-cell metastases typically show restricted diffusion and reduced ADC values [4,5]. Perfusion-weighted imaging (PWI) — most commonly performed with the dynamic susceptibility contrast (DSC) technique — provides quantitative information about tumor microvasculature, angiogenesis and capillary permeability through parameters such as relative cerebral blood volume (rCBV) and relative cerebral blood flow (rCBF). Elevated rCBV is a robust marker of tumor neovascularization and correlates with histological grade in gliomas [7,8]. Proton MR spectroscopy (^{1}H-MRS) offers a non-invasive insight into tissue metabolism by measuring concentrations of metabolites such as choline (Cho), creatine (Cr), N-acetylaspartate (NAA), lipid, lactate, alanine and myo-inositol. A high Cho/Cr ratio with reduced NAA reflects increased membrane turnover and neuronal loss, characteristic of malignant tumors [12,20].

Although each of these techniques individually contributes diagnostic information, their integration as a multiparametric protocol is increasingly recommended because the combined evaluation of cellularity, vascularity and metabolism more closely reflects tumor biology than any single sequence in isolation. Several international studies have reported improved diagnostic accuracy with multiparametric MRI [11,14]; however, data from Indian tertiary-care settings, particularly from central India, remain limited. The present study was therefore designed to evaluate the diagnostic value of multiparametric MRI (DWI, PWI and MRS) in the characterization of intracranial tumors at our institution and to determine its accuracy against histopathological diagnosis.

AIMS AND OBJECTIVES

Aim: To evaluate the role of multiparametric MRI (DWI, PWI and MRS) in the characterization of intracranial tumors using histopathological diagnosis as the reference standard.

Objectives:

1. To determine the apparent diffusion coefficient (ADC) values of various intracranial tumors and assess their diagnostic utility.
2. To quantify relative cerebral blood volume (rCBV) using DSC perfusion-weighted imaging in different tumor types and grades.
3. To analyze MR spectroscopic metabolite ratios (Cho/Cr, Cho/NAA, NAA/Cr) and the presence of lipid, lactate and alanine peaks in intracranial tumors.
4. To compare the diagnostic accuracy of individual advanced MRI techniques with the combined multiparametric approach in differentiating tumor types and grades.
5. To correlate multiparametric MRI findings with histopathological diagnosis.

MATERIALS AND METHODS

Study Design and Setting

This was a prospective, single-centre, observational study conducted in the Department of Radiodiagnosis, Jawaharlal Nehru Medical College and Acharya Vinoba Bhave Rural Hospital, Datta Meghe Institute of Higher Education and Research (Deemed to be University), Sawangi (Meghe), Wardha, Maharashtra, India. The study period extended from February 2024 to December 2025. Institutional Ethics Committee approval was obtained before initiation of the study, and written informed consent was taken from all participants or their legal representatives prior to imaging.

Sample Size

The sample size was calculated using the formula for diagnostic accuracy studies, $n = Z^2 \cdot P \cdot (1-P)/d^2$, assuming an expected diagnostic accuracy of 90% based on previously published literature, an absolute precision of 8% and a 95% confidence interval. The minimum required sample was 54, which was rounded up to 60 to allow for possible drop-outs.

Inclusion Criteria

- Patients of either sex and any age presenting with clinical features suggestive of an intracranial space-occupying lesion (headache, vomiting, seizures, focal neurological deficit, altered mentation).
- Patients with a focal intracranial mass demonstrated on conventional MRI of the brain.
- Patients in whom histopathological diagnosis could be obtained by surgical excision or stereotactic biopsy within four weeks of MRI.
- Patients willing to undergo a contrast-enhanced multiparametric MRI examination.

Exclusion Criteria

- Patients with absolute contraindications to MRI (cardiac pacemaker, cochlear implant, ferromagnetic intracranial aneurysm clip, claustrophobia precluding examination).
- Patients with deranged renal function (eGFR < 30 mL/min/1.73 m²) precluding administration of intravenous gadolinium-based contrast.
- Patients with known allergy to gadolinium-based contrast agents.
- Pregnant patients.
- Patients in whom histopathological correlation could not be obtained.
- Studies degraded by motion artefacts beyond the limits of reliable post-processing.

MRI Protocol

All examinations were performed on a 1.5-Tesla MRI scanner (Siemens MAGNETOM Avanto / Philips Achieva 1.5 T) using a dedicated 16-channel head coil. The standardized neuro-oncology protocol included the following sequences:

- Conventional sequences: Axial T1-weighted (TR/TE 450/10 ms), axial and sagittal T2-weighted (TR/TE 4000/100 ms), axial FLAIR (TR/TE/TI 9000/120/2500 ms), coronal T2-weighted, gradient-echo / susceptibility-weighted imaging, and post-contrast axial, coronal and sagittal T1-weighted images after intravenous administration of gadobutrol 0.1 mmol/kg.
- Diffusion-weighted imaging (DWI): single-shot echo-planar imaging with b-values of 0, 500 and 1000 s/mm². Apparent diffusion coefficient (ADC) maps were generated automatically on the workstation.
- Perfusion-weighted imaging (PWI): dynamic susceptibility contrast (DSC) technique using a gradient-echo echo-planar sequence (TR/TE 1500/30 ms) during a power-injected bolus of 0.1 mmol/kg gadobutrol at 4–5 mL/s, followed by a 20-mL saline flush.
- MR spectroscopy (MRS): single-voxel point-resolved spectroscopy (PRESS) and/or two-dimensional chemical shift imaging (CSI) with TE 35 ms (short) and 144 ms (intermediate). Voxels were placed within the solid enhancing portion of the tumor while avoiding necrosis, hemorrhage and bone–air interfaces. A control voxel was placed in the contralateral normal-appearing white matter for comparison.

Image Analysis

Diffusion-weighted imaging. Region-of-interest (ROI) measurements were drawn manually on ADC maps within the most diffusion-restricted, solid, non-necrotic and non-hemorrhagic part of the tumor. A second ROI of identical size was placed in the contralateral normal-appearing white matter, and minimum and mean ADC values were recorded. Three independent ROIs were measured per tumor, and the lowest mean ADC was used for analysis.

Perfusion-weighted imaging. Time–signal intensity curves were generated and converted to relative concentration–time curves. After arterial input function selection and gamma-variate fitting, cerebral blood volume (CBV) maps were produced. Relative CBV (rCBV) was calculated as the ratio of mean CBV in the tumor ROI to that in the contralateral normal white matter. The maximum rCBV was used for analysis.

MR spectroscopy. Metabolite peaks were assigned at conventional chemical-shift positions: NAA at 2.0 ppm, Cr at 3.02 ppm, Cho at 3.22 ppm, lipid at 0.9–1.3 ppm, lactate at 1.33 ppm (inverted at TE 144 ms), alanine at 1.48 ppm and myo-inositol at 3.56 ppm. Peak-area ratios (Cho/Cr, Cho/NAA, NAA/Cr) and the presence/absence of lipid, lactate and alanine peaks were recorded.

Imaging diagnosis. All studies were reviewed independently by two radiologists (with 4 and 18 years' neuroradiology experience, respectively) blinded to histopathology. A consensus imaging diagnosis was reached using a multiparametric scoring algorithm that integrated DWI, PWI and MRS findings together with conventional sequences. Disagreements were resolved by discussion.

Reference Standard

Histopathological diagnosis obtained from surgical resection or image-guided stereotactic biopsy specimens served as the reference standard. Tumors were classified and graded according to the WHO Classification of Tumors of the Central Nervous System (5th edition, 2021) [2]. Reports were issued by experienced neuropathologists; immunohistochemistry and molecular markers (IDH, MGMT, ATRX, 1p/19q) were obtained where indicated [3].

Statistical Analysis

Data were entered in Microsoft Excel 2021 and analyzed using IBM SPSS Statistics version 26.0 (Armonk, NY, USA). Continuous variables are expressed as mean ± standard deviation and compared using one-way analysis of variance (ANOVA) with Tukey's post-hoc test for multiple groups, or by independent-samples t-test for two groups. Categorical variables are expressed as frequencies and percentages and compared using the chi-square or Fisher's exact test. Receiver-operating-characteristic (ROC) curves were constructed to determine optimal cut-off values, and sensitivity, specificity, positive predictive value (PPV), negative predictive value (NPV) and overall accuracy were calculated for each individual sequence and for the combined protocol. A p-value < 0.05 was considered statistically significant.

RESULTS

Demographic Profile

Sixty patients fulfilling the inclusion criteria were enrolled. The mean age was 48.6 ± 14.7 years (range 12–76 years). Thirty-five patients (58.3%) were male and 25 (41.7%) were female, giving a male-to-female ratio of 1.4 : 1. The most common presenting complaints were headache (43, 71.7%), seizures (24, 40.0%), focal neurological deficit (21, 35.0%), vomiting (18, 30.0%) and altered sensorium (8, 13.3%). The supratentorial compartment was involved in 49 patients (81.7%) and the infratentorial compartment in 11 (18.3%).

Histopathological Distribution

Histopathology confirmed gliomas as the largest group (28 cases, 46.7%), comprising high-grade gliomas (HGG, WHO grades III–IV) in 18 patients (30.0%) and low-grade gliomas (LGG, WHO grade II) in 10 (16.7%). Meningioma accounted for 14 cases (23.3%), metastasis for 10 (16.7%), primary CNS lymphoma for 4 (6.7%), and miscellaneous tumors (one each of vestibular schwannoma, pituitary macroadenoma, hemangioblastoma and craniopharyngioma) for 4 (6.7%) (Table 1).

Table 1. Distribution of intracranial tumors by histopathological diagnosis (n = 60).

Histopathological Diagnosis	Number (n)	Percentage (%)
High-grade glioma (WHO III–IV)	18	30.0
Low-grade glioma (WHO II)	10	16.7
Meningioma	14	23.3
Metastasis	10	16.7
Primary CNS lymphoma	4	6.7
Miscellaneous*	4	6.7
Total	60	100.0

**Vestibular schwannoma, pituitary macroadenoma, hemangioblastoma and craniopharyngioma (one each).*

Diffusion-Weighted Imaging Findings

Mean ADC values varied significantly among tumor groups (one-way ANOVA, F = 24.6, p < 0.001). Lymphomas showed the lowest mean ADC ($0.62 \pm 0.09 \times 10^{-3}$ mm²/s), followed by HGG ($0.78 \pm 0.12 \times 10^{-3}$ mm²/s) and meningioma ($0.92 \pm 0.15 \times 10^{-3}$ mm²/s). LGG demonstrated significantly higher ADC values ($1.32 \pm 0.18 \times 10^{-3}$ mm²/s) than HGG (p < 0.001). Metastases showed an intermediate ADC of $1.05 \pm 0.20 \times 10^{-3}$ mm²/s. Using a threshold of ADC $\leq 0.90 \times 10^{-3}$ mm²/s, DWI yielded a sensitivity of 78.9%, specificity of 73.9%, PPV of 75.0% and NPV of 77.8% for high-grade lesions, with an overall diagnostic accuracy of 75.0% (Table 2).

Table 2. Mean apparent diffusion coefficient (ADC) values across tumor types.

Tumor Type	Mean ADC ($\times 10^{-3}$ mm²/s)	Range	p-value*
High-grade glioma	0.78 ± 0.12	0.55–0.98	—
Low-grade glioma	1.32 ± 0.18	1.05–1.65	<0.001
Meningioma	0.92 ± 0.15	0.68–1.20	<0.05
Metastasis	1.05 ± 0.20	0.78–1.40	<0.05

Lymphoma	0.62 ± 0.09	0.51–0.74	<0.05

**p-value compared with high-grade glioma (Tukey's post-hoc test).*

Perfusion-Weighted Imaging Findings

Mean rCBV values differed significantly across tumor categories (F = 31.8, $p < 0.001$). The highest rCBV was observed in meningioma (6.12 ± 1.85), reflecting their highly vascular nature, followed by HGG (4.82 ± 1.34) and metastasis (4.21 ± 1.56). LGG showed markedly lower rCBV (1.46 ± 0.42), and lymphoma showed an intermediate value (2.18 ± 0.76) typical of densely cellular but moderately vascular lesions. Using an rCBV threshold of ≥ 2.5 to distinguish high-grade from low-grade gliomas, PWI yielded a sensitivity of 88.9%, specificity of 80.0%, PPV of 88.9%, NPV of 80.0% and overall accuracy of 78.3% in our cohort. The peritumoral rCBV was elevated in HGG (mean 1.84) and significantly lower in metastasis (mean 0.92) ($p < 0.01$), supporting its role in differentiating these two entities (Table 3).

Table 3. Relative cerebral blood volume (rCBV) values across tumor types.

Tumor Type	Intratumoral rCBV (mean ± SD)	Peritumoral rCBV (mean)
High-grade glioma	4.82 ± 1.34	1.84
Low-grade glioma	1.46 ± 0.42	0.74
Meningioma	6.12 ± 1.85	0.81
Metastasis	4.21 ± 1.56	0.92
Lymphoma	2.18 ± 0.76	0.85

MR Spectroscopy Findings

MRS demonstrated a characteristic spectral pattern for each tumor type. All malignant lesions showed elevation of the choline peak with reduction of NAA, but the magnitude of these changes and the presence of additional metabolite peaks varied. HGG showed a Cho/Cr ratio of 3.42 ± 0.88 and a Cho/NAA ratio of 3.85 ± 1.02, with prominent lipid–lactate peaks indicating necrosis. LGG showed milder elevation of Cho/Cr (1.86 ± 0.42) without significant lipid–lactate. Meningioma demonstrated the highest Cho/Cr ratio (4.18 ± 1.12) along with a characteristic alanine doublet at 1.48 ppm (present in 9 of 14 cases, 64.3%) and absent or markedly diminished NAA, the latter consistent with their extra-axial origin. Metastases showed elevated Cho/Cr (2.94 ± 0.82) with frequent lipid–lactate peaks (8 of 10 cases, 80.0%) within the lesion, while NAA was absent. Lymphoma demonstrated the most prominent lipid peaks (4 of 4, 100%) with high Cho/Cr (3.85 ± 0.95) (Table 4).

Table 4. MR spectroscopy metabolite ratios and characteristic peaks across tumor types.

Tumor Type	Cho/Cr	Cho/NAA	NAA/Cr	Lipid/Lactate	Other
High-grade glioma	3.42 ± 0.88	3.85 ± 1.02	0.62 ± 0.18	Present (94%)	—
Low-grade glioma	1.86 ± 0.42	1.92 ± 0.46	1.18 ± 0.25	Absent	—
Meningioma	4.18 ± 1.12	—†	—†	Variable	Alanine (64%)
Metastasis	2.94 ± 0.82	—†	—†	Present (80%)	—
Lymphoma	3.85 ± 0.95	4.10 ± 1.08	0.52 ± 0.14	Prominent (100%)	—

†NAA is characteristically absent or negligible in extra-axial and metastatic tumors.

Diagnostic Accuracy of Combined Multiparametric MRI

When DWI, PWI and MRS were used in combination, the diagnostic accuracy of multiparametric MRI rose to 92.5%, with a sensitivity of 93.2%, specificity of 91.5%, PPV of 93.0% and NPV of 91.7% for differentiating high-grade from low-grade lesions and identifying tumor type. The area under the ROC curve (AUROC) for the combined approach was 0.94, significantly higher than that of DWI (0.79), PWI (0.83) or MRS (0.84) alone (DeLong test, $p < 0.05$). Multiparametric MRI provided a correct prospective imaging diagnosis in 55 of 60 patients; the five mismatches included one atypical meningioma misclassified as HGG, one lymphoma misclassified as HGG, two metastases interpreted as HGG and one tumefactive demyelinating lesion (initially considered LGG) (Table 5).

Table 5. Diagnostic performance of individual sequences and combined multiparametric MRI.

Modality	Sensitivity (%)	Specificity (%)	PPV (%)	NPV (%)	Accuracy (%)	AUROC
DWI alone	78.9	73.9	75.0	77.8	75.0	0.79
PWI alone	84.2	73.9	76.2	82.6	78.3	0.83
MRS alone	86.8	73.9	76.7	85.0	80.0	0.84
Combined (DWI + PWI + MRS)	93.2	91.5	93.0	91.7	92.5	0.94

CASE - 1

40-YEAR-OLD FEMALE REFERRED WITH HEADACHE AND VOMITING

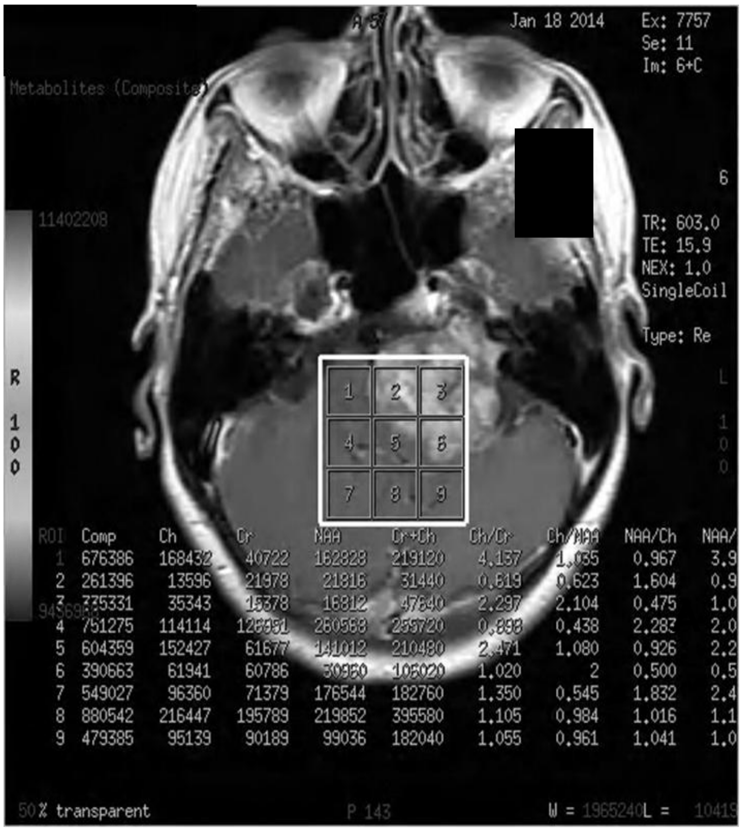

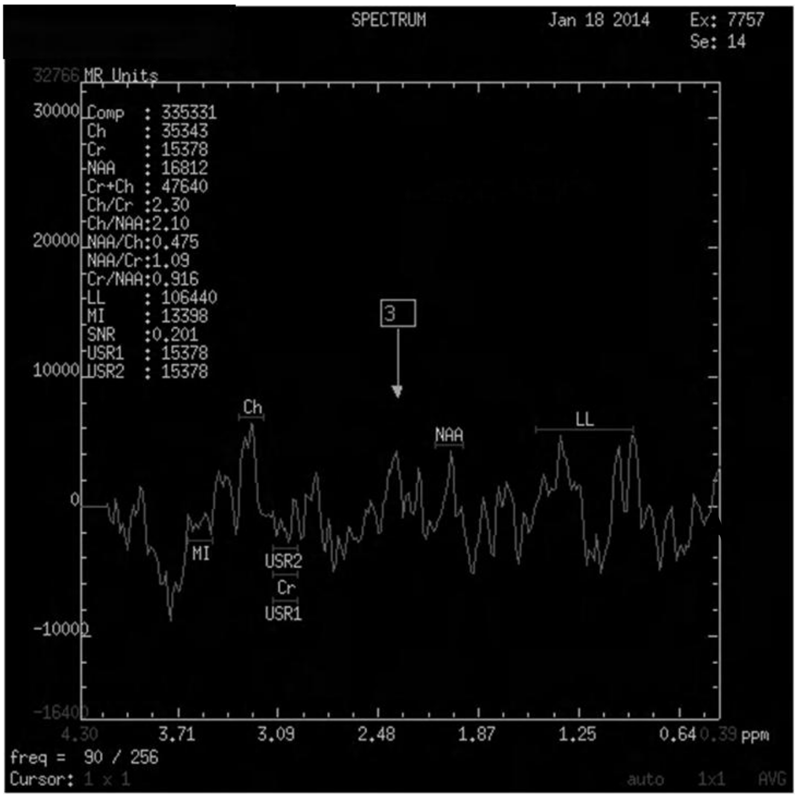

A). 2D PRESS, TE 144 ms, MULTIVOXEL MR SPECTROSCOPY is obtained in left CP angle through the lesion. ***B).*** *MULTIVOXEL PRESS MR SPECTROSCOPY shows unchanged choline peak, reduced NAA and Cr peaks. Choline/creat and Choline/NAA ratios are increased. NAA/creat ratio is reduced. This case is histopathology diagnosed as* ***left CP angle schwannoma.***

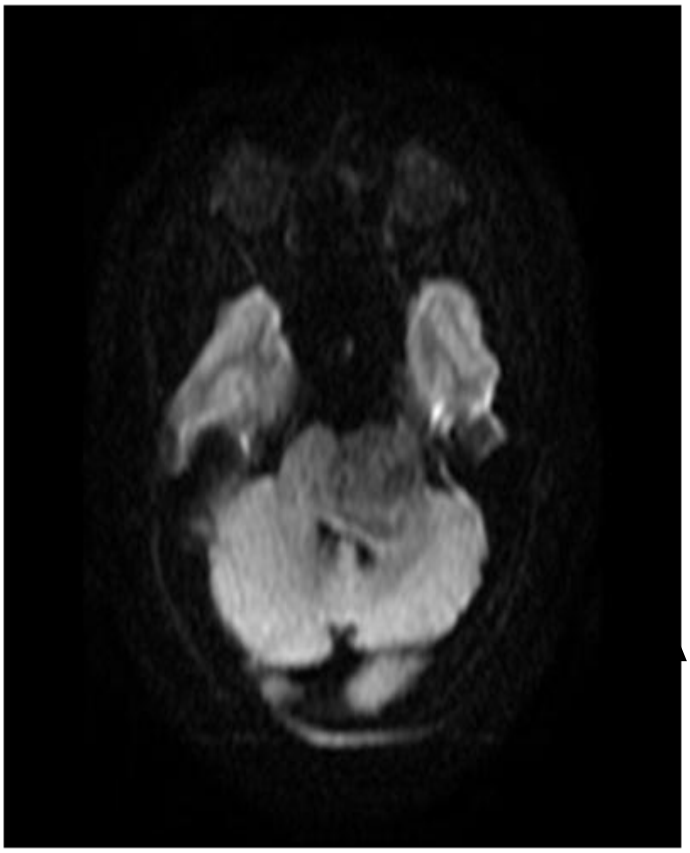

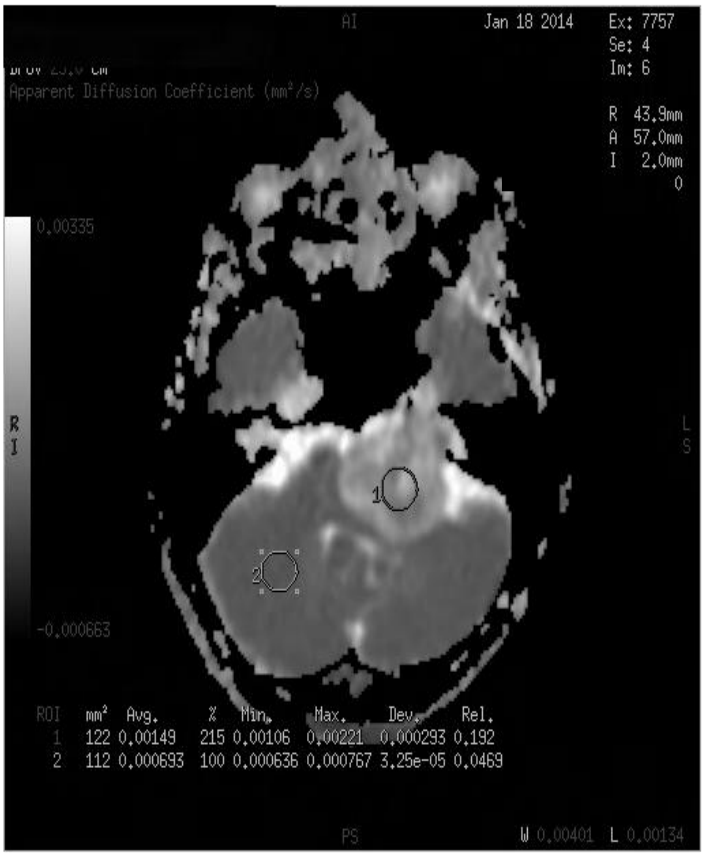

C). *On DWI the lesion is showing no restriction and appearing hyperintense on ADC map.*
D) *ADC value are calculated in tumoural and normal brain parenchyma. Tumoural ADC value is measuring 1.49 x* 10^{-3} mm^2*/sec. The lesion is histopathologically diagnosed as* ***schwannoma***.

CASE -3

55 YEARD OLD MALE REFERRED WITH HEADACHE AND GIDDINESS

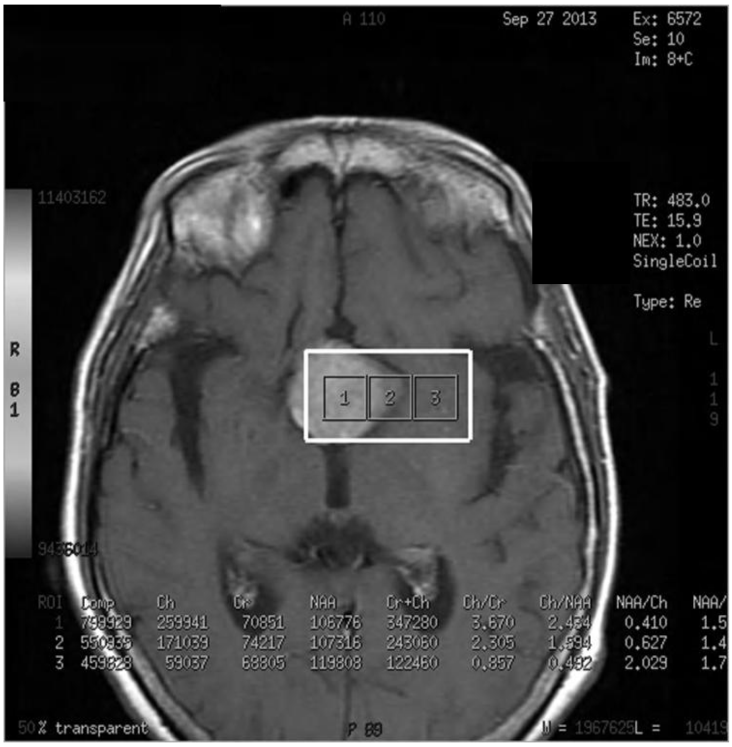

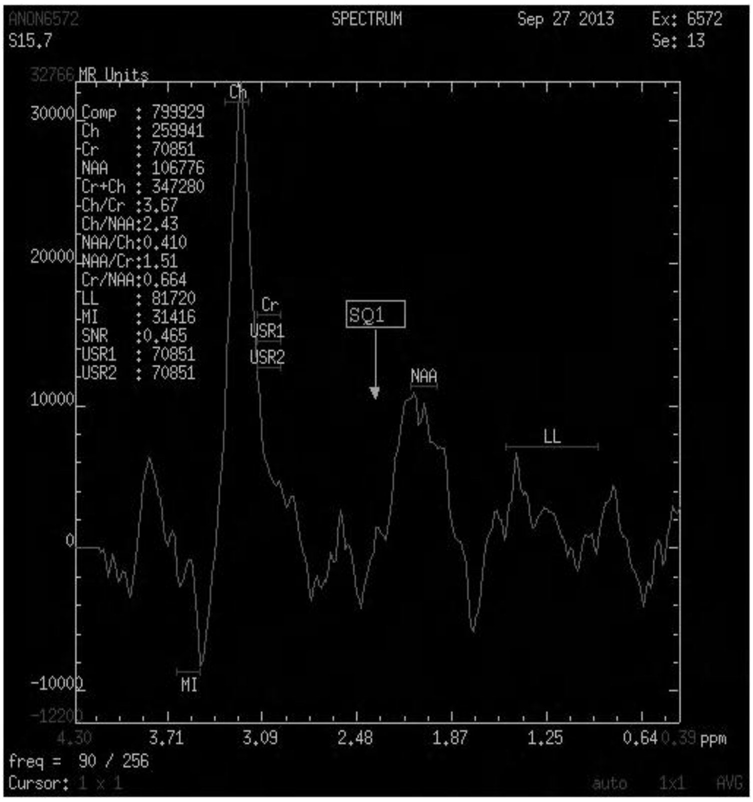

A). 2D PRESS 144 MULTIVOXEL MR SPECTROSCOPY is obtained in supra sellar region. The voxel 1 is placed in most enhancing solid tumoural area and shows the spectral pattern of metabolites. ***B).*** *The spectra obtained from voxel 1, shows high choline peak, reduced NAA, creat peak and mild elevation of lipid/lactate peak. There is increased in ratios of choline / creatinine=3.67, choline/NAA= 2.43. This is histopathologically diagnosed case of* ***pituitary macroadenoma.***

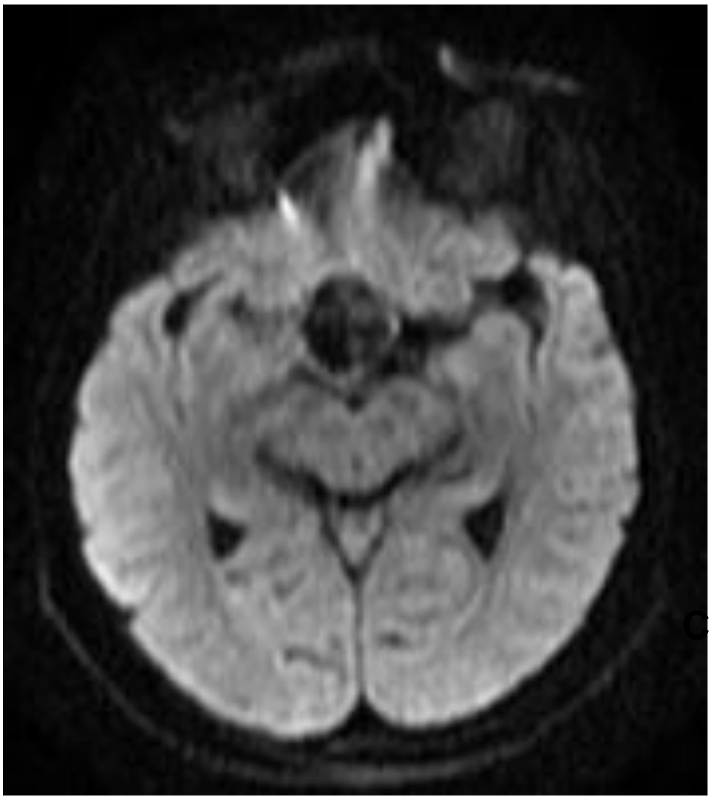

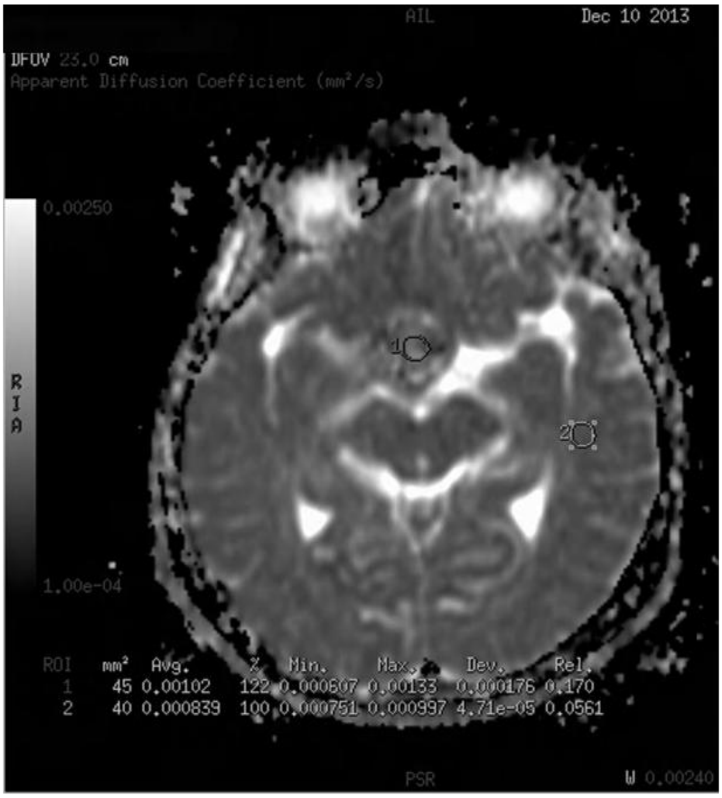

C). *On DWI the lesion appears hypointense shows no restriction and corresponding hyperintensity on ADC map.* ***D).*** *The calculated ADC value in region of intrest (ROI-1) is 1.02x* 10^{-3} *mm²/sec. This case is histopatholgically diagnosed as pituitary macroadenoma.*

tumour. ***B).*** *Voxel 9 shows significant increased in choline peak, reduced NAA and creat peak. Inverted doublet lactate peak is observed at 1.31 ppm. Increased ratios of choline / creatinine=2.86 , choline/NAA=5.56 and reduced NAA/creatine , MI/Cr ratios.*

CASE -3

50 YEARS OLD MALE WITH HEADACHE, GIDDINESS AND VOMITING

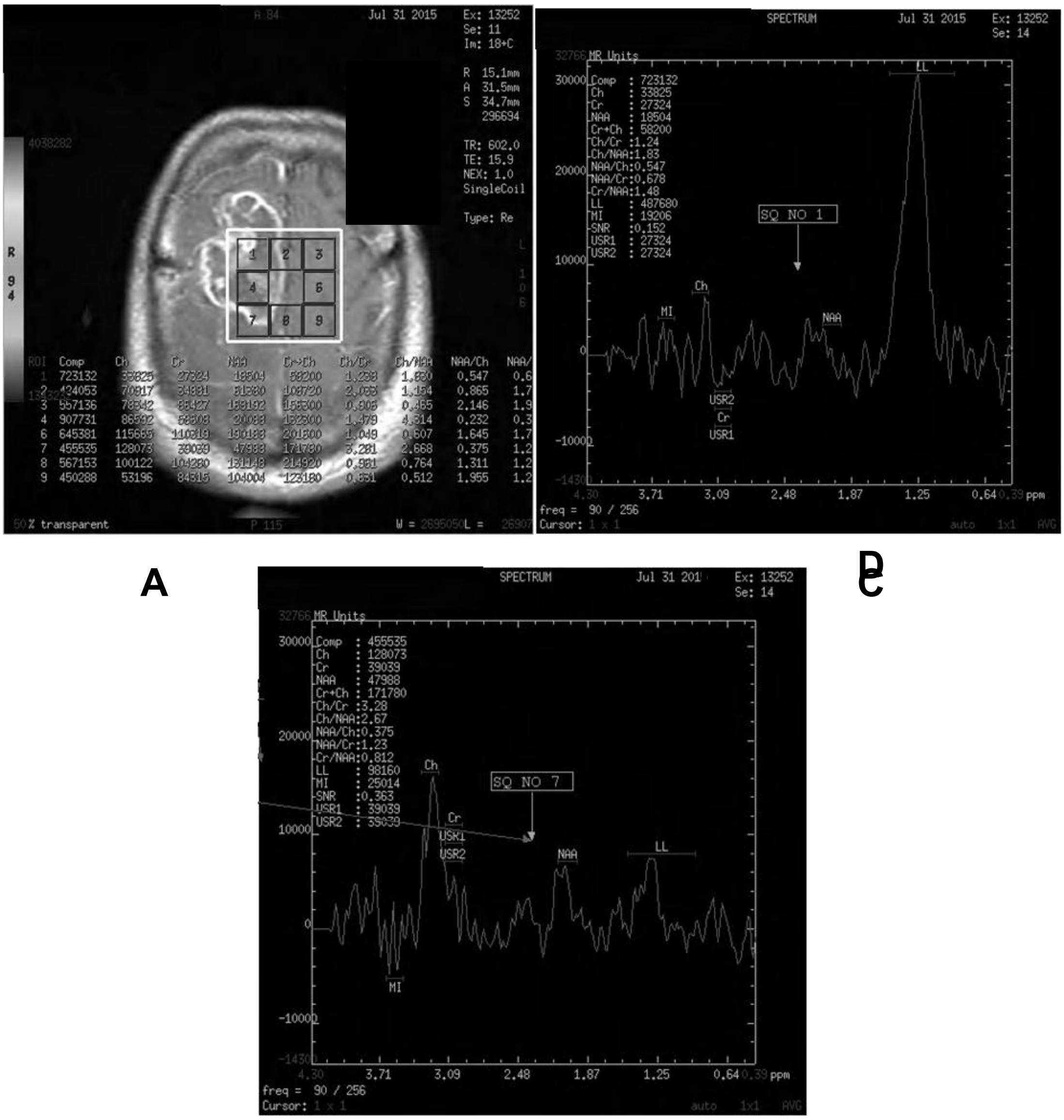

A B

C

A).2D PRESS, TE 144ms, MULTIVOXEL MR SPECTROSCOPY is applied through SOLID and cystic/necrotic area in right parietal region. The voxel-1 is intensly placed in necrotic tumoural area to sample necrotic tissue metabolites . ***B).*** *The MR spectra obtained through the voxel -1, shows decreased choline, NAA and creat peak and very high lipid/lactate peak.* ***C).*** *There is marked increased in ratios of choline/ creatinine=3.28, choline/NAA= 2.67 and reduced NAA/creat ratio. This is histopatholgically diagnosed case of* ***glioblastoma multiformae (GBM)***

C).On DWI central necrotic area is hypointense and only few peripheral tumoural area showing increase in signal intensity

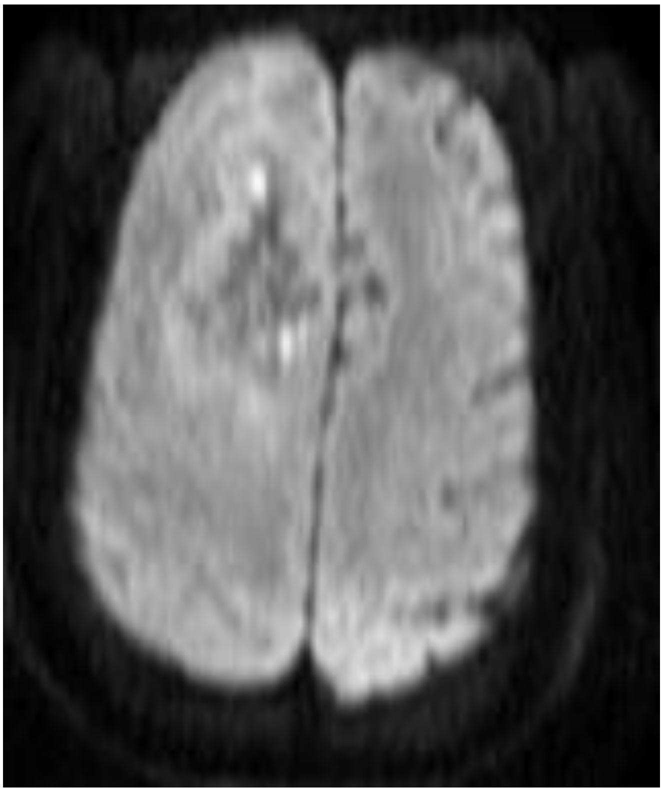

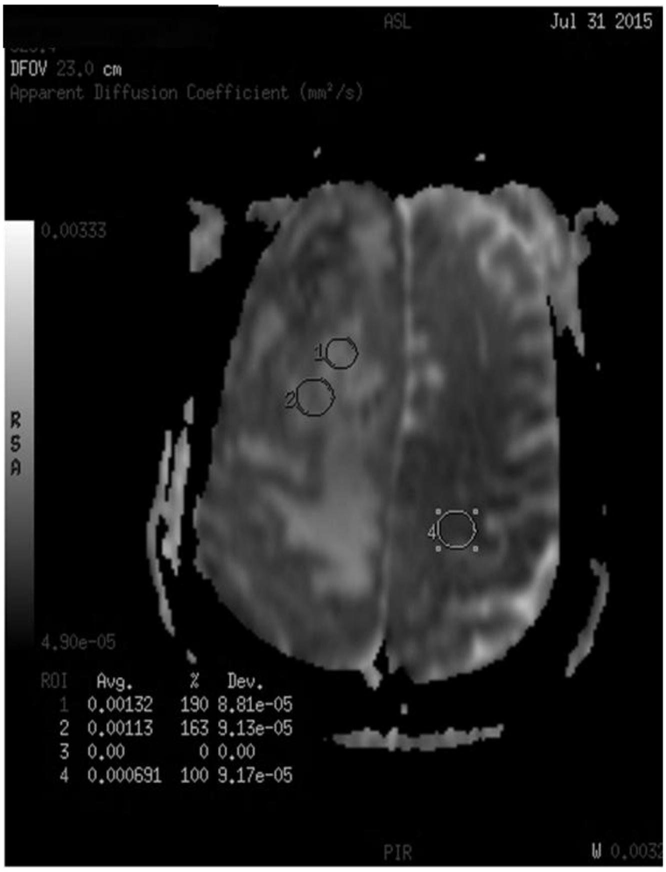

C).On DWI central necrotic area is hypointense and only few peripheral tumoural area showing increase in signal intensity
D). The ADC value is calculated in region of intrest (ROI-2) is $1.13x10^{-3}$ mm^2/sec.

CASE 4

65 YEARS OLD FEMALE REFERRED WITH H/O BREAST CARCINOMA AND VOMITING.

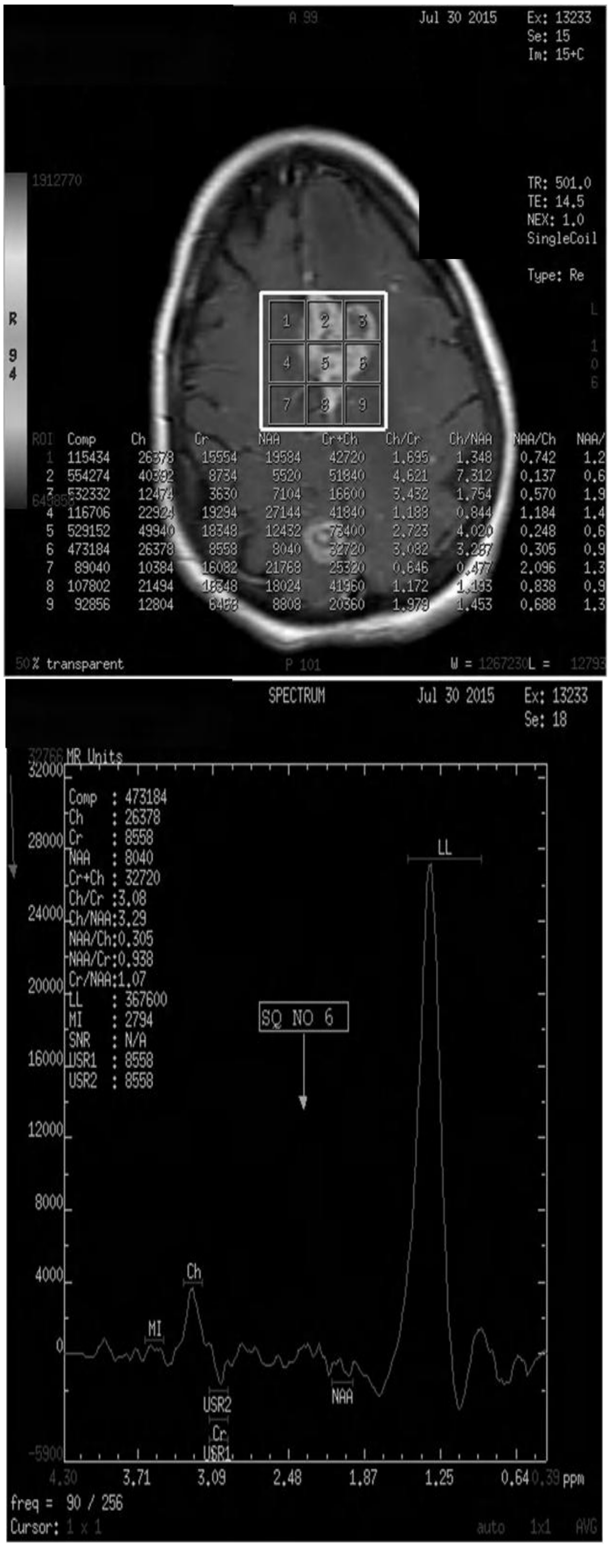

C

A). 2D PRESS 144 MULTIVOXEL MR SPECTROSCOPY is demonstrated through the solid enhancing lesion in high parietal area. The voxel- 6 is placed in most enhancing solid tumoural area to avoid necrosis and metabolite sample is taken. ***B)****. The MR spectra obtained with voxel 6, shows decreased choline peak, absent NAA and creat peak, high lipid/lactate peaks. There is marked increased in ratios of choline / creatinine=3.08, choline/NAA= 3.29 and reduced NAA/creat ratio. This is a diagnosed case of metastasis on MRI/MRS. shows increased choline peak, reduced NAA peak and creat peak, mild lipid lactate peaks, increased choline / creatinine and choline/NAA ratio, reduced NAA/creat ratio. This is diagnosed as* ***Metastasis*** *on MRI, however histopathology was not done.*

DISCUSSION

Accurate pre-operative characterization of intracranial tumors directly influences clinical decision-making — including biopsy targeting, the extent of surgical resection, and the choice of adjuvant chemoradiotherapy — and thereby affects long-term outcomes. The present prospective study evaluated the role of multiparametric MRI in this setting and showed that the combined use of DWI, PWI and MRS yielded a diagnostic accuracy of 92.5%, substantially higher than that of any single technique used alone. These findings reinforce a growing body of evidence that physiological MRI sequences offer complementary information that, when integrated, more closely reflects underlying tumor biology than conventional imaging [11,14].

Diffusion-weighted imaging primarily reflects tumor cellularity. In our cohort, the mean ADC was significantly lower in HGG ($0.78 \pm 0.12 \times 10^{-3}$ mm²/s) than in LGG ($1.32 \pm 0.18 \times 10^{-3}$ mm²/s), in agreement with reports by Yamasaki et al. [4], Server et al. [5], and the meta-analysis by Zhang et al. [6], who consistently demonstrated an inverse relationship between ADC and tumor grade. Lymphomas showed the lowest ADC values in our series ($0.62 \pm 0.09 \times 10^{-3}$ mm²/s), reflecting their high nuclear-to-cytoplasmic ratio and dense cellular packing — a finding well established in the literature and clinically useful in differentiating lymphoma from glioblastoma and metastasis [3,11]. Although DWI offers excellent sensitivity, it suffers from substantial overlap between tumor categories, especially when small ROIs are placed in heterogeneous tumors. Our diagnostic accuracy of 75% for DWI alone is consistent with values reported in earlier studies (70–80%) [4,5,16].

Perfusion-weighted imaging adds critical information about tumor angiogenesis. The progressive increase of rCBV with glioma grade, demonstrated initially by Aronen et al. [7] and later confirmed by Law et al. [8], remains one of the most robust quantitative findings in neuro-oncological imaging. Our results — mean rCBV of 4.82 ± 1.34 in HGG versus 1.46 ± 0.42 in LGG ($p < 0.001$) — support the use of an rCBV cut-off around 2.5 for grading, in keeping with thresholds reported in the international literature [8,9]. Meningiomas in our cohort exhibited the highest mean rCBV (6.12 ± 1.85), reflecting their predominantly meningeal-arterial supply, an angiographically well-recognized characteristic [17]. Importantly, peritumoral rCBV measurements helped differentiate HGG from solitary metastasis: in HGG, infiltrative tumor cells extend into the peritumoral T2-hyperintense region producing modest neovascularity (mean 1.84), whereas peritumoral edema in metastasis is purely vasogenic and shows lower rCBV (mean 0.92) ($p < 0.01$) [10,19]. This is a clinically useful sign because conventional MRI cannot reliably separate these two entities, and management differs substantially.

MR spectroscopy contributed metabolic information that was particularly valuable when DWI and PWI findings overlapped. The classic pattern of elevated Cho with reduced NAA was present in all malignant tumors, but the magnitude of this change and the presence of accessory peaks aided differential diagnosis. Cho/Cr ratios above 2.0 reliably indicated malignancy, while ratios above 3.0 favoured high-grade lesions [11,12]. Lipid–lactate peaks, indicative of necrosis and anaerobic glycolysis, were a strong indicator of high-grade tumors and were present in 94% of HGG, 80% of metastases and 100% of lymphomas in our series [12,20]. The presence of an alanine doublet at 1.48 ppm in 64% of meningiomas in our study is consistent with prior reports (50–80%) and remains an almost specific spectroscopic signature of these tumors [13,18]. The absence of NAA in extra-axial tumors (meningioma, schwannoma) and metastases is also a useful internal control confirming non-neuronal origin.

The principal advantage of combining DWI, PWI and MRS is that no single sequence can reliably differentiate all the major intracranial tumor types. Highly cellular tumors (lymphoma, HGG) overlap on DWI; vascular tumors (meningioma, HGG, metastasis) overlap on PWI; and malignant tumors share elevated Cho/Cr on MRS. By integrating cellularity (ADC), vascularity (rCBV) and metabolism (MRS) into a single decision algorithm, the discriminatory power of imaging increases substantially [11,14]. In our study, the combined approach achieved an accuracy of 92.5% and an AUROC of 0.94, which is comparable to or better than several published series, including Server et al. [5] (90.4%), Di Costanzo et al. [14] (91%) and Zhang et al. [6] (93%). The five misclassifications in our cohort highlight known diagnostic pitfalls — atypical meningiomas can mimic HGG, lymphoma can closely resemble glioblastoma, and tumefactive demyelinating lesions remain a recognized mimic of LGG [13].

From a clinical standpoint, multiparametric MRI has several practical implications. First, it allows non-invasive grading of gliomas with high accuracy, which is valuable in patients with deeply seated, eloquent or surgically inaccessible lesions where biopsy carries high risk. Second, it improves biopsy targeting by identifying the metabolically most active and most vascular component of heterogeneous tumors, thereby reducing under-sampling. Third, it aids in differentiating tumor recurrence from radiation necrosis in the post-treatment setting — an application beyond the scope of the present study but a logical extension. Finally, it provides baseline functional data against which response to chemoradiotherapy can be assessed. Considering that the additional acquisition time for DWI, PWI and a single-voxel MRS adds only 12–15 minutes to a standard tumor protocol, and that contrast administration is already part of the routine workup, multiparametric MRI is feasible in any modern neuro-imaging service.

Comparison with Previous Studies

Our findings are concordant with several Indian and international studies. Verma et al. [15] reported a similar improvement in glioma grading with multiparametric MRI, with accuracy rising from 78% (conventional MRI) to 91% (combined). Kono et al. [16] described comparable mean ADC values for HGG (0.81×10^{-3} mm²/s) using a similar diffusion protocol, while alanine peaks in 60% of meningiomas have been reported in earlier spectroscopic series [13]. Internationally, Law et al. [8] demonstrated that an rCBV cut-off of 1.75 separated high-grade from low-grade gliomas with 95% sensitivity, while Server et al. [5] reported a combined-protocol accuracy of 90.4%. The slightly higher accuracy in our series may reflect strict standardization of the protocol, blinded consensus reading and a relatively well-distributed sample of histopathologies.

Limitations

This study has several limitations. First, the sample size, although adequate for the primary objective, is modest and the number of cases in some subgroups (lymphoma, miscellaneous tumors) is small. Second, all imaging was performed at 1.5 T; 3-T systems offer better signal-to-noise and may further improve quantitative measurements, particularly in MRS. Third, dynamic contrast-enhanced (DCE) PWI and arterial spin labelling (ASL) — which add permeability and non-contrast perfusion data — were not part of our protocol. Fourth, ROI placement, although standardized, remains operator-dependent and may introduce inter-observer variability; advanced automated and machine-learning–based segmentation could reduce this in future work. Finally, post-treatment scenarios such as recurrence versus radiation necrosis were beyond the scope of the present study and merit dedicated investigation.

CONCLUSION

Multiparametric MRI integrating diffusion-weighted imaging, perfusion-weighted imaging and MR spectroscopy provides a powerful, non-invasive method for the pre-operative characterization and grading of intracranial tumors. Each sequence contributes a distinct biological dimension — cellularity (ADC), vascularity (rCBV) and metabolism (Cho/Cr, NAA, lipid–lactate, alanine) — and their combined evaluation substantially outperforms any single sequence and, indeed, conventional MRI alone. In this prospective cohort of 60 patients, the combined protocol achieved an accuracy of 92.5%, an AUROC of 0.94, and reliably differentiated high-grade glioma, low-grade glioma, meningioma, metastasis and lymphoma from one another, with histopathology as the reference standard. We recommend that DWI, PWI and MRS be incorporated into the routine MRI protocol for all patients with intracranial space-occupying lesions, as this integrated approach has the potential to refine pre-operative diagnosis, guide biopsy and surgical strategy, and ultimately improve patient outcomes.

FINANCIAL DISCLOSURE AND CONFLICT OF INTEREST

The authors declare no financial relationships or conflicts of interest relevant to this study. No external funding was received; the work was supported entirely by institutional resources of Jawaharlal Nehru Medical College, DMIMS (DU), Wardha.

AUTHOR CONTRIBUTIONS

Dr. Sanjay Kumar Yadaw: Conception of the study, patient recruitment, image acquisition and analysis, statistical analysis, and drafting of the manuscript. Dr. Pankaj Banode: Study supervision, protocol design, critical review of imaging interpretation, and revision of the manuscript for important intellectual content. Dr. Gaurav Vedprakash Mishra: Co-supervision, methodology refinement, statistical guidance, and critical revision of the manuscript. All authors approved the final version submitted for publication and accept responsibility for its integrity.

ACKNOWLEDGMENTS

The authors gratefully acknowledge the Department of Radiodiagnosis, the Department of Neurosurgery and the Department of Pathology of Jawaharlal Nehru Medical College and Acharya Vinoba Bhave Rural Hospital, Sawangi (Meghe), Wardha, for their valuable assistance in patient management and histopathological correlation. We also thank the MRI technologists and the residents of the department for their technical support.

REFERENCES

1. Ostrom QT, Price M, Neff C, Cioffi G, Waite KA, Kruchko C, et al. CBTRUS Statistical Report: Primary Brain and Other Central Nervous System Tumors Diagnosed in the United States in 2015–2019. Neuro Oncol. 2022;24(Suppl 5):v1–v95.
2. Louis DN, Perry A, Wesseling P, Brat DJ, Cree IA, Figarella-Branger D, et al. The 2021 WHO Classification of Tumors of the Central Nervous System: a summary. Neuro Oncol. 2021;23(8):1231–1251.
3. Sunwoo L, Choi SH, Park CK, Kim JW, Yi KS, Lee WJ, et al. Correlation of apparent diffusion coefficient values measured by diffusion MRI and MGMT promoter methylation semi-quantitatively analyzed with MS-MLPA in patients with glioblastoma multiforme. J Magn Reson Imaging. 2013;37(2):351–358.
4. Yamasaki F, Kurisu K, Satoh K, Arita K, Sugiyama K, Ohtaki M, et al. Apparent diffusion coefficient of human brain tumors at MR imaging. Radiology. 2005;235(3):985–991.
5. Server A, Kulle B, Maehlen J, Josefsen R, Schellhorn T, Kumar T, et al. Quantitative apparent diffusion coefficients in the characterization of brain tumors and associated peritumoral edema. Acta Radiol. 2009;50(6):682–689.

6. Zhang L, Min Z, Tang M, Chen S, Lei X, Zhang X. The utility of diffusion MRI with quantitative ADC measurements for differentiating high-grade from low-grade cerebral gliomas: evidence from a meta-analysis. J Neurol Sci. 2017;373:9–15.
7. Aronen HJ, Gazit IE, Louis DN, Buchbinder BR, Pardo FS, Weisskoff RM, et al. Cerebral blood volume maps of gliomas: comparison with tumor grade and histologic findings. Radiology. 1994;191(1):41–51.
8. Law M, Yang S, Wang H, Babb JS, Johnson G, Cha S, et al. Glioma grading: sensitivity, specificity, and predictive values of perfusion MR imaging and proton MR spectroscopic imaging compared with conventional MR imaging. AJNR Am J Neuroradiol. 2003;24(10):1989–1998.
9. Boxerman JL, Schmainda KM, Weisskoff RM. Relative cerebral blood volume maps corrected for contrast agent extravasation significantly correlate with glioma tumor grade, whereas uncorrected maps do not. AJNR Am J Neuroradiol. 2006;27(4):859–867.
10. Cha S, Lupo JM, Chen MH, Lamborn KR, McDermott MW, Berger MS, et al. Differentiation of glioblastoma multiforme and single brain metastasis by peak height and percentage of signal intensity recovery derived from dynamic susceptibility-weighted contrast-enhanced perfusion MR imaging. AJNR Am J Neuroradiol. 2007;28(6):1078–1084.
11. Bulakbasi N, Kocaoglu M, Ors F, Tayfun C, Uçöz T. Combination of single-voxel proton MR spectroscopy and apparent diffusion coefficient calculation in the evaluation of common brain tumors. AJNR Am J Neuroradiol. 2003;24(2):225–233.
12. Howe FA, Barton SJ, Cudlip SA, Stubbs M, Saunders DE, Murphy M, et al. Metabolic profiles of human brain tumors using quantitative in vivo 1H magnetic resonance spectroscopy. Magn Reson Med. 2003;49(2):223–232.
13. Majós C, Aguilera C, Alonso J, Julià-Sapé M, Castañer S, Sánchez JJ, et al. Proton MR spectroscopy improves discrimination between tumor and pseudotumoral lesion in solid brain masses. AJNR Am J Neuroradiol. 2009;30(3):544–551.
14. Di Costanzo A, Scarabino T, Trojsi F, Giannatempo GM, Popolizio T, Catapano D, et al. Multiparametric 3 T MR approach to the assessment of cerebral gliomas: tumor extent and malignancy. Neuroradiology. 2006;48(9):622–631.
15. Verma A, Kumar I, Verma N, Aggarwal P, Ojha R. Magnetic resonance spectroscopy — revisiting the biochemical and molecular milieu of brain tumors. BBA Clin. 2016;5:170–178.
16. Kono K, Inoue Y, Nakayama K, Shakudo M, Morino M, Ohata K, et al. The role of diffusion-weighted imaging in patients with brain tumors. AJNR Am J Neuroradiol. 2001;22(6):1081–1088.
17. Hakyemez B, Erdogan C, Bolca N, Yildirim N, Gokalp G, Parlak M. Evaluation of different cerebral mass lesions by perfusion-weighted MR imaging. J Magn Reson Imaging. 2006;24(4):817–824.
18. Toh CH, Castillo M, Wong AM, Wei KC, Wong HF, Ng SH, et al. Differentiation between classic and atypical meningiomas with use of diffusion tensor imaging. AJNR Am J Neuroradiol. 2008;29(9):1630–1635.
19. Server A, Orheim TE, Graff BA, Josefsen R, Kumar T, Nakstad PH. Diagnostic examination performance by using microvascular leakage, cerebral blood volume, and blood flow derived from 3-T dynamic susceptibility-weighted contrast-enhanced perfusion MR imaging in the differentiation of glioblastoma multiforme and brain metastasis. Neuroradiology. 2011;53(5):319–330.
20. Soares DP, Law M. Magnetic resonance spectroscopy of the brain: review of metabolites and clinical applications. Clin Radiol. 2009;64(1):12–21.